

PROCESSING AND BREAKDOWN LOCALIZATION RESULTS FOR AN L-BAND STANDING-WAVE CAVITY *

Faya Wang and Chris Adolphsen, SLAC, Menlo Park, CA 94025, U.S.A.

Abstract

An L-band (1.3 GHz), normal-conducting, 5-cell, standing-wave cavity that was built as a prototype capture accelerator for the ILC is being high-power processed at SLAC. The goal is to demonstrate stable operation at 15 MV/m with 1 msec, 5 Hz pulses and the cavity immersed in a 0.5 Tesla solenoidal magnetic field. This paper summarizes the performance that was ultimately achieved and describes a novel analysis of the modal content of the stored energy in the cavity after a breakdown to determine on which iris it occurred.

INTRODUCTION

A half-length (5-cell) prototype π -mode standing-wave cavity was built at SLAC to verify that the relatively high gradient (15 MV/m) required for efficient positron capture can be reliably achieved with the long (1.0 ms) ILC pulses [1 2 3]. Figure 1 shows a cross section of the cavity, whose design was complicated by the extensive cooling required to prevent significant detuning from average rf heating during its 5 Hz operation.

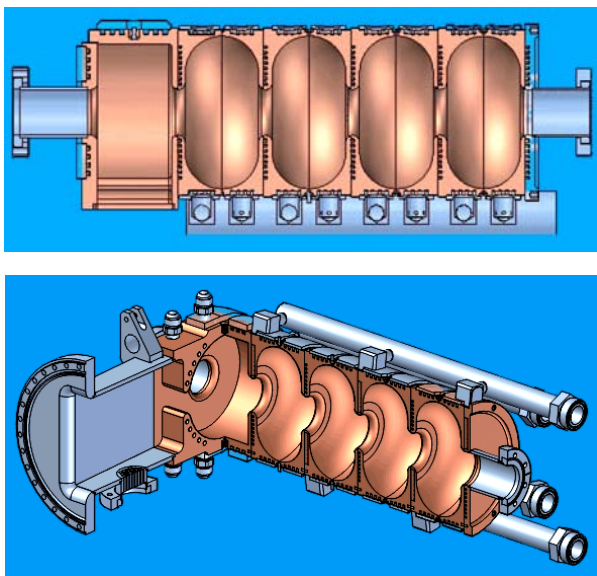


Figure 1: Cross sectional view of the 5-cell cavity where the coupler cell is on the left and an rf probe (not shown) is located in the beam pipe just outside the right-most cell. Cooling water circulates through rectangular grooves in the irises and outer cavity walls.

A single bunch about 20 pC (very small beam loading) was accelerated at 5 Hz in the cavity at NLCTA at different injection times (175 μ s and 610 μ s) during rf pulses with different widths (180 μ s and 1050 μ s). These

combinations were chosen to distinguish detuning effects from low average heating, high average heating and intra-pulse heating. The gradients inferred from the bunch energy gains are plotted in Fig 2 versus the net cavity input power, which is limited by modulator. As expected, there are no significant gradient changes.

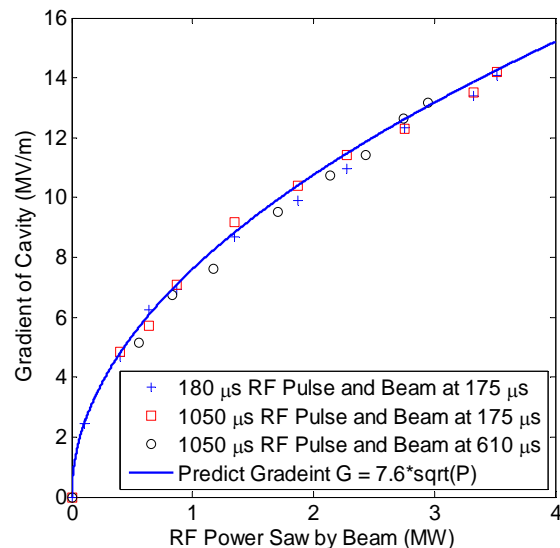


Figure 2: Gradient prediction and measurement with single bunch versus the net cavity input power (forward – reflected) for different pulse widths and bunch injection times.

After about 1000 hrs conditioning, for 1ms rf pulse the cavity has reached average gradient of 13.7 MV/m with and without 0.5 Tesla solenoid field. And the breakdown rate at this gradient is typically 1/hr for both cases when running at 5 Hz with 1 ms pulses.

Although the cavity reached the design gradient, it incurred several thousand breakdowns during rf processing. Interestingly, the subsequent decay times of the stored energy, measured with an rf probe located in the beam pipe just after the last cell at the downstream end of the cavity (i.e., the end opposite of the power coupler), varied greatly from event to event, taking from a few μ s to over 15 μ s to decrease by 20 dB. Also, there appeared to be a beating pattern during the decays, all of which suggests that the breakdowns (probably on the irises) were causing the RF energy to be isolated in the downstream cells, and that the trapped energy was being partitioned among the resulting modes of those cells. This prompted a study of the cavity modes with an equivalent circuit model to see if the predicted decay spectra for various numbers of isolated downstream cells match the data spectra, thus identifying the likely irises on which the breakdowns had occurred.

* Work Supported by DOE Contract DE-AC03-76F00515.

BREAKDOWN LOCATION IN THE CAVITY

Measurements of ions emitted during breakdown in a 30 GHz structure show their maximum velocity to be about $1e4$ m/s [4]. If the velocities are similar in the ILC cavity, then the plasma generated by rf breakdown would spread out on the order of 1 cm in $1 \mu\text{s}$, which is small compared to the 10 cm iris spacing but more significant compared to the 3 cm iris radius. So on this timescale, the largest plasma effect may be to reduce the coupling through the irises in which the breakdown occurs. This will be assumed in the following analysis, and is supported by other observations that are described below.

To simulate the effect of a breakdown on a particular iris with the equivalent circuit model, the cell-to-cell coupling through that iris was set to zero after the fields reached steady state in the π -mode. The model shows that the stored energy remaining in each section of the now divided cavity will excite all possible modes in that section to some degree. As these modes decay, the amplitude of the store energy shows a beating pattern that depends on the frequency differences. Figure 3 shows plots of the Fourier Transform (FT) of the log of the simulated probe power (no phase information is used) in the downstream section during a $10 \mu\text{s}$ period after different irises are blocked. In the case where no irises are blocked, the initial field in the first cell was assumed to be 3 percent lower than others to produce a noticeable beating. For other cases, the initial fields in the cells were assumed to be equal, which may not be the case just after breakdown due to the loading of breakdown-generated currents.

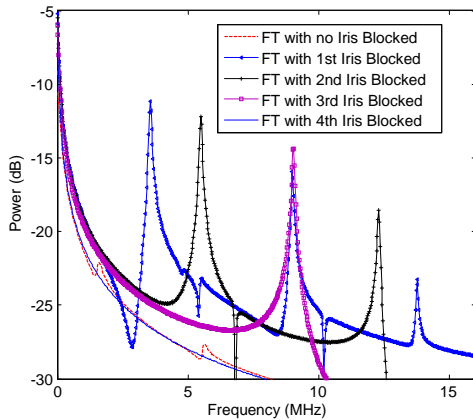


Figure 3: Predicted frequency spectrum of the log of the probe power at the downstream end of the cavity when different irises are blocked and the cell fields are equal initially, except for the no iris blocked case, in which the first cell has a field 3% lower than the others.

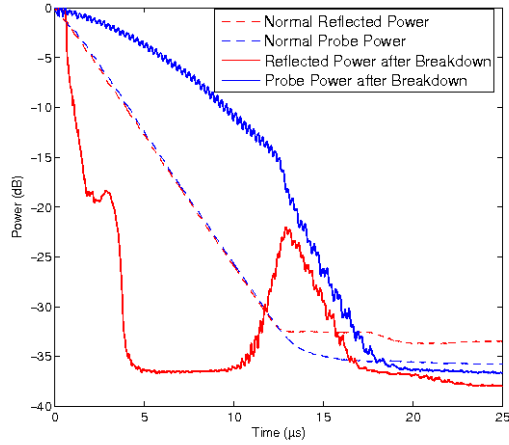
In Figures 4 waveform data is a typical example of what is interpreted as breakdowns on first of the four irises. The waveform data shown in the figure were taken with a 100 MHz sampling scope that started ($t = 0$) shortly after the main input power was shutoff (which

occurred about $1 \mu\text{s}$ after a fault was detected). Both the reflected and probe power are normalized to 0 dB at this point, as are these values for the non-breakdown event that are shown with dashed lines in the figures (in this case, the two curves track each other as expected for the critical coupling cavity). For the breakdown events, the reflected power decreases very fast, but has a profile that is complicated by the fact that the input power was first reduced by about 20 dB before $t = 0$ and then was fully shut off a few μs later through a different mechanism. In Figure 4a, for example, there is a ‘ledge’ in the reflected power curve at about -20 dB for a few μs before it falls to the measurement noise level at around -35 dB. In contrast, the probe power, which is a measure of stored energy, decreases relatively slowly, and shows that the breakdown was effective at isolating the downstream portion of the cavity. In fact, the probe power decay rate is about half the nominal rate (i.e., roughly consistent with Q0) so the isolating mechanism does not itself absorb much power (although for the other examples, it does decrease faster).

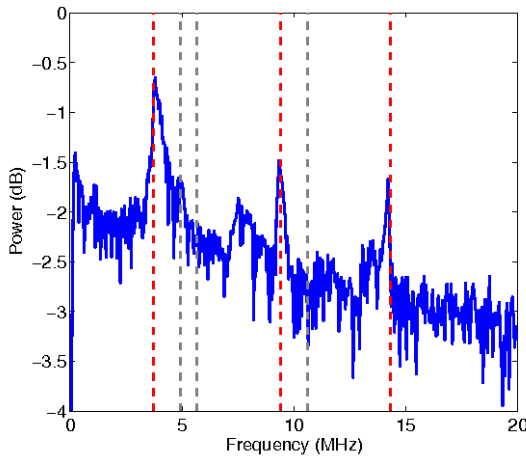
Another interesting feature of the data in Figure 4 is the eventual turn on the reflected power that then tracks the decay of the probe power after $t = 13 \mu\text{s}$. The mechanism that was isolating the stored energy appears to be no longer effective and so the energy flows out through the coupler and appears as reflected power. The timescale for this transition is similar to that observed in X-band structures[5], and suggests the effect is a function of the plasma only (e.g., the recombination time of the ions and electrons).

Figures 4 also include plots of the FT of the log of the probe power computed over the time ranges noted in the figure captions. The red-dashed vertical lines are those corresponding to the peaks in Figure 3 (in which it is assumed the isolated cells have equal fields initially), and the gray-dashed vertical lines are all possible additional beating frequencies. The good agreement of the data peaks with those in Figure 3 suggests the breakdown in this case is isolating the stored energy in the downstream four cells. However, it is not clear why the data peaks are less pronounced than in the simulations (and correspondingly, the simulated probe power signal has much higher peak-to-valley variations than the data). In Figure 4c, a similar FT comparison is made, but this time with the 12-18 μs data after the reflected power turns on again. In this case, the vertical lines are for the full five cell cavity with the downstream four cells having equal fields initially and the coupler cell having zero field initially. The match of the vertical lines to the data peaks is consistent with the un-blocking of the first iris.

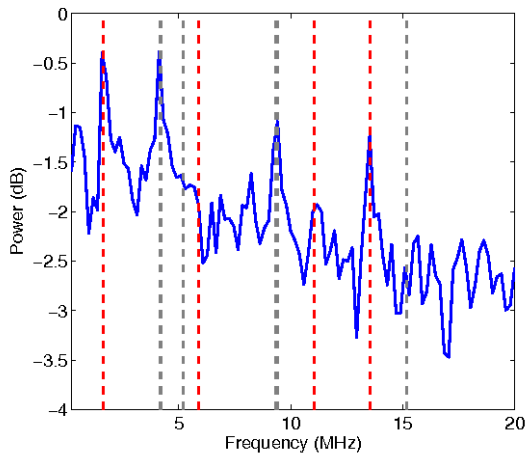
All observed events map into one of five patterns of breakdown noted above where the FT peaks of the data match those of the predictions if the isolated cells essentially have equal fields initially. The fact that all possible iris patterns are seen during experiment supports the assumption that the breakdowns do not significantly detune the neighboring cells. Hence, the peak probe spectra provide a unique signature that is likely indicating the iris on which the breakdown occurred.



(a)



(b)



(c)

Figure 4: (a) The blue and red dashed lines are the probe power and reflected power, respectively, when the cavity discharges at the end of the pulse (no breakdown), and the solid lines are these waveforms for a breakdown event where the time scale has been shifted so $t = 0$ aligns with the beginning of the normal discharge. (b) The FT of the log of the probe power in the 0-12 μs time range (blue solid line), and the peak spectral frequencies in the simulated measurement in the case where the first

iris is blocked (the vertical red lines correspond to the resulting peak frequencies when the initial fields are equal in each cell when k is zeroed, and the grey vertical lines are the other possible beating frequencies). (c) Same as (b) but for the 12-18 μs data, and the case where no irises are blocked in the simulation but only the downstream four cells are filled initially.

SUMMARY

The 5-cell, 1.3 GHz cavity built as a prototype for the ILC positron capture accelerator has achieved gradient of 13.7 MV/m with and without 0.5 Tesla solenoid field, when running at 5 Hz with 1 ms pulses, however the breakdown rate of 1/hr is quite high for both cases. The gradient measurement verified that there is no significant detune the designed cooling when running at high average rf power ($\sim 4\text{kW}/\text{cell}$).

This cavity is a useful test bed to explore breakdown phenomena in SW cavities. To aid this study, an equivalent circuit was established. For breakdown events, it was assumed that the cavity is isolated at a given iris and the stored energy is then partitioned into the modes of the reduced number of cells. The peaks in the probe power spectrum from breakdown events match the patterns predicted by the model with this assumption. Thus, such a comparison appears to provide a means of localizing the breakdowns, which is generally hard to do in SW cavities. If more probes could be added to the cavities (e.g., one in each cell), perhaps the details of the plasma evolution could be better understood.

ACKNOWLEDGEMENTS

We wish to thank Juwen Wang, Zenghai Li, Chris Nantista, Erik Jongewaard, Gordon Bowden and the ARD Test Facilities Group for their efforts on the design, construction, cold testing and high power operation of this cavity.

REFERENCES

- [1] J.W. Wang et al., SLAC Report No. SLAC-PUB-12412,2007.
- [2] J.W. Wang et al., SLAC Report No. SLAC-PUB-11767,2006.
- [3] F. Wang, C. Adolphsen, and J. Wang, SLAC Report No. SLAC-PUB-13459, 2008.
- [4] J.W. Wang and G. A. Loew, SLAC Report No. SLACPUB-4647,1988.
- [5] C. Adolphsen (unpublished).